中国科学院高能物理研究所
Institute of High Energy Physics Chinese Academy of Sciences

中国科学院
CHINESE ACADEMY OF SCIENCES

“2024年粲强子物理研讨会”

The polarization puzzle in $D^0 \to VV$ and its implications in $D^0 \to V\gamma$

Presenter: Ye Cao (曹叶)

Division of Theoretical Physics

Institute of High Energy Physics, CAS

Based on Phy.Rev.D 109(2024)7,073002 and arXiv:2311.05249 (PRD in press)

In collaboration with Qiang Zhao (赵强) and Yin Cheng (程茵)

2024/05/11 河南郑州

Outline

1. Background of $D^0 \to VV$
2. Formalism: tree-level short-distance transition vs. long-distance final state interactions.
3. Numerical results and discussions
4. Extension: $D^0 \to V\gamma$
5. Summary

1. Background

pQCD → (leading) → Helicity Conservation → Longitudinal polarization dominant for $D^0 \to VV$

For an exclusive decay, the longitudinal polarization fraction is defined as $f_L \equiv \frac{BR^{longi}}{BR^{longi}+BR^{trans}}$.
The longitudinal polarization dominance (LPD) means $f_L \simeq 1$.

- In the beauty sector, naïve power counting predicts that $B \to VV$ $(V = \phi, K^*, \rho, \omega)$ decays are LPD since the helicity-flip transition is suppressed at the order of Λ_{QCD}/m_b.

Brodsky et.al., Phys. Rev. D, 24 :2848, 1981.
Chernyak et al., Nucl. Phys. B, 201:492, 1982.

In most cases, the exp. measurements support the LPD phenomenon, e.g. $B^0 \to \rho^+\rho^-, B^+ \to \rho^0\rho^+, \rho^0 K^{*+}$.
But tensions exit in $B \to \phi K^*$.

Bernard Aubert et al., PRL91,171802 (2003).
K. F. Chen et al., PRL91, 201801 (2003).

■ In the charm sector, the situation is more complicated.

□ Apparent deviations of the LPD are observed in experiment, such as $f_L = (0.00 \pm 0.10 \pm 0.08)$ for $D^0 \to \phi\omega$; $f_L = (71 \pm 4 \pm 2)\%$ for $D^0 \to \rho^0\rho^0$; transverse polarization dominance for $D^0 \to \overline{K}^{*0}\rho^0$.

BES-III Collaboration, Phys. Rev. Lett., 128(1):011803, 2022 .
FOCUS Collaboration, Phys. Rev. D, 75:052003, 2007.
MARK-III Collaboration, Phys. Rev. D, 45:2196–2211, 1992.

□ The naïve factorization model and the Lorentz invariant-based symmetry model indeed predict that the longitudinal polarization faction may not be dominant in $D \to VV$.

A. N. Kamal et al., PRD43, 843 (1991)
Ian Hinchlie and Thomas A. Kaeding, PRD54, 914 (1996)
Paulo F. Bedaque et al., PRD49, 269 (1994)
Manfred Bauer, B. Stech, and M. Wirbel, Z. Phys. C34, 103 (1987)
Hai-Yang Cheng and Cheng-Wei Chiang, PRD81, 114020 (2010)
Hua-Yu Jiang, Fu-Sheng Yu, Qin Qin, Hsiang-nan Li, and Cai-Dian Lyu, Chin. Phys. C42, 063101 (2018)

Non-perturbative mechanism may become essentially important. But how to quantify it?

short-distance transitions:

Direct emission

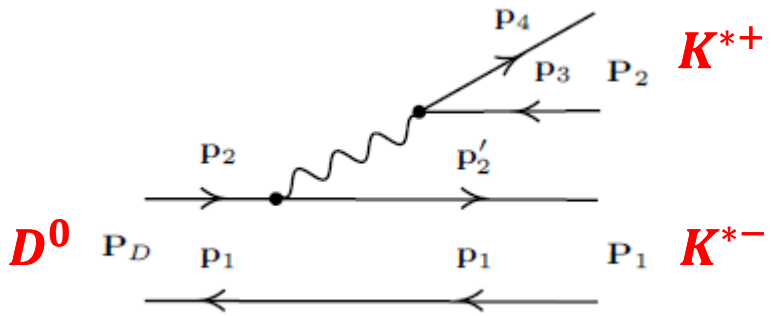

Color suppressed

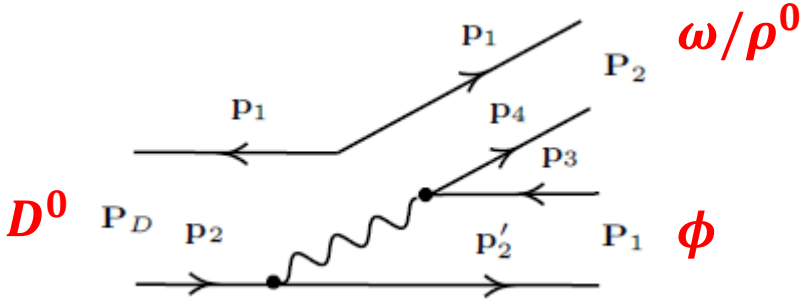

At the leading order, one would expect $Br(D^0 \to \phi\rho^0) \simeq Br(D^0 \to \phi\omega)$.

$$u\bar{u} = \frac{1}{2}(u\bar{u} + d\bar{d}) + \frac{1}{2}(u\bar{u} - d\bar{d}) = \frac{1}{\sqrt{2}}(\omega + \rho^0)$$

Internal conversion

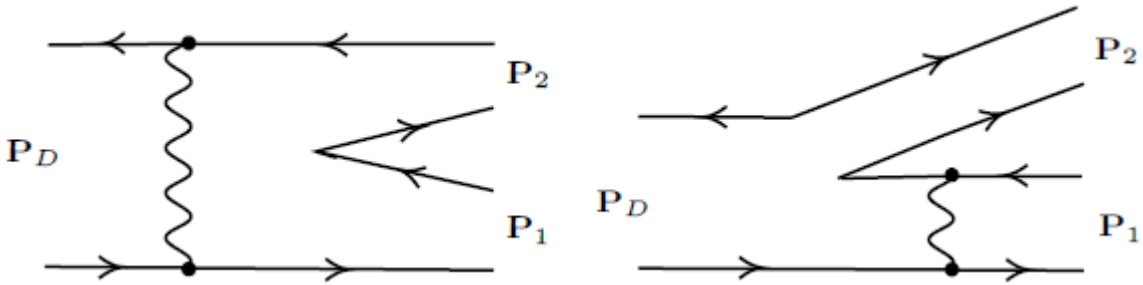

BES-III Collaboration, Phys. Rev. Lett., 128(1):011803 (2022)
P. d'Argent et al., JHEP, 05:143 (2007)

Significant differences arise from the experimental measurements:

(I) Negligibly small longitudinal polarization with the $\phi\omega$ channel:

$$f_L = 0.00 \pm 0.10 \pm 0.08$$

which corresponds to $f_L < 0.24$ at 95% C.L.

(II) Dominance of the S-wave in $D^0 \to \phi\rho^0$ suggests relatively large f_L.

(III) Difference in b.r.s:

$$Br^{exp}(D^0 \to \phi\rho^0) = (1.56 \pm 0.13) \times 10^{-3}$$
$$Br^{exp}(D^0 \to \phi\omega) \simeq (0.65 \pm 0.10) \times 10^{-3}$$

There must be mechanisms beyond the leading tree-level transitions.

Amplitudes for $D^0 \to VV$ via the short-distance dynamics.

Decay channels	Amplitudes
$K^{*-}\rho^+$	$[g^{(\mathrm{P})}_{\mathrm{DE}} + e^{i\theta} g^{(\mathrm{P})}_{\mathrm{IC}(s\bar{d})}] V_{cs} V_{ud}$
$\bar{K}^{*0}\rho^0$	$\frac{1}{\sqrt{2}} [g^{(\mathrm{P})}_{\mathrm{CS}} - e^{i\theta} g^{(\mathrm{P})}_{\mathrm{IC}(s\bar{d})}] V_{cs} V_{ud}$
$\bar{K}^{*0}\omega$	$\frac{1}{\sqrt{2}} [g^{(\mathrm{P})}_{\mathrm{CS}} + e^{i\theta} g^{(\mathrm{P})}_{\mathrm{IC}(s\bar{d})}] V_{cs} V_{ud}$
$K^{*+}K^{*-}$	$[g^{(\mathrm{P})}_{\mathrm{DE}} + e^{i\theta} g^{(\mathrm{P})}_{\mathrm{IC}(s\bar{s})}] V_{cs} V_{us}$
$K^{*0}\bar{K}^{*0}$	$e^{i\theta} [g^{(\mathrm{P})}_{\mathrm{IC}(s\bar{s})} V_{cs} V_{us} + g^{(\mathrm{P})}_{\mathrm{IC}(d\bar{d})} V_{cd} V_{ud}]$
$\rho^+\rho^-$	$[g^{(\mathrm{P})}_{\mathrm{DE}} + e^{i\theta} g^{(\mathrm{P})}_{\mathrm{IC}(d\bar{d})}] V_{cd} V_{ud}$
$\rho^0\rho^0$	$\frac{1}{2} [-g^{(\mathrm{P})}_{\mathrm{CS}} + e^{i\theta} g^{(\mathrm{P})}_{\mathrm{IC}(d\bar{d})}] V_{cd} V_{ud}$
$\omega\omega$	$\frac{1}{2} [g^{(\mathrm{P})}_{\mathrm{CS}} + e^{i\theta} g^{(\mathrm{P})}_{\mathrm{IC}(d\bar{d})}] V_{cd} V_{ud}$
$\rho^0\omega$	$-\frac{1}{2} e^{i\theta} g^{(\mathrm{P})}_{\mathrm{IC}(d\bar{d})} V_{cd} V_{ud}$
$\phi\rho^0$	$\frac{1}{\sqrt{2}} g^{(\mathrm{P})}_{\mathrm{CS}} V_{cs} V_{us}$
$\phi\omega$	$\frac{1}{\sqrt{2}} g^{(\mathrm{P})}_{\mathrm{CS}} V_{cs} V_{us}$

- Notice that the $K^{*+}K^{*-}$ channel has large b.r. due to the direct emission process.
- $2m_{K^*} \sim m_\phi + m_\rho \sim m_\phi + m_\omega$
- Long distance transition mechanism due to the $K^*\bar{K}^*$ final-state interactions (FSIs) should be considered:
- Moreover, FSIs involving other intermediate meson rescatterings can also contribute. A systematic treatment is required.

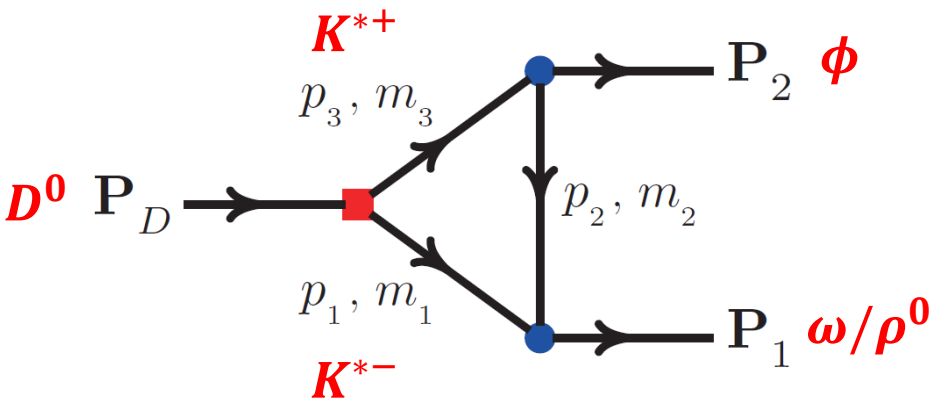

2. Tree-level short-distance transitions vs. long-distance final state interactions

- Taking $D^0 \to \phi\rho^0/\phi\omega$ as an example, the tree-level amplitude reads:

$$i\mathcal{M}_{(\mathrm{P})}(D^0 \to \phi\rho^0/\phi\omega)$$
$$= \langle\phi\rho^0/\phi\omega|\phi(u\bar{u})\rangle\langle\phi(u\bar{u})|H^{(\mathrm{CS})}_{W(\mathrm{P})}|D_0\rangle = \frac{1}{\sqrt{2}} g^{(\mathrm{P})}_{\mathrm{CS}} V_{cs}V_{us}$$

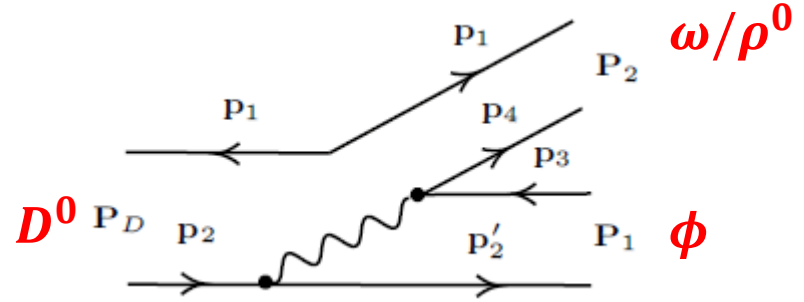

- The amplitude due to the intermediate $K^{*+}K^{*-}$ rescatterings can be written as:

$$i\mathcal{M}^{loop}_{(\mathrm{P})\phi\rho^0} = \frac{1}{\sqrt{2}} g^{(\mathrm{P})}_{\mathrm{DE}} V_{cs}V_{us} \sum_{(\mathbb{K})} \tilde{\mathcal{I}}[(\mathrm{P}); K^{*+}, K^{*-}, (\mathbb{K})]$$

$$i\mathcal{M}^{loop}_{(\mathrm{P})\phi\omega} = \left(\frac{1}{\sqrt{2}} g^{(\mathrm{P})}_{\mathrm{DE}} + e^{i\delta} g^{(\mathrm{P})}_{\mathrm{IC}(s\bar{s})}\right) V_{cs}V_{us}$$
$$\times \sum_{(\mathbb{K})} \tilde{\mathcal{I}}[(\mathrm{P}); K^{*+}, K^{*-}, (\mathbb{K})] \ ,$$

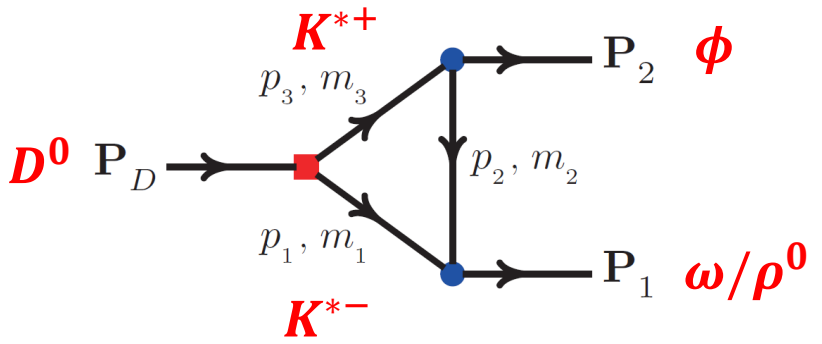

"P" can be either "PC" or "PV" for parity-conserving or parity-violating amplitudes.

Different strange particle exchanges in $K^{*+}K^{*-} \to \phi\rho^0/\phi\omega$.

Long-distance amplitudes via the FSIs

For instance, the loop amplitude for the kaon exchange can be expressed as

$$\tilde{\mathcal{I}}[(\mathrm{PC}); K^{*+}, K^{*-}, (K)]$$
$$= \int \frac{d^4p_1}{(2\pi)^4} V_{1\mu\nu} D^{\mu\mu'}(K^*) V_{2\mu'} D(K) V_{3\nu'} D^{\nu\nu'}(\bar{K}^*) \mathcal{F}(p_i^2)$$

with the vertex couplings:

$$\begin{cases} V_{1\mu\nu} = -ig_{DK^*\bar{K}^*}\epsilon_{\alpha\beta\mu\nu}p_1^\alpha p_3^\beta, \\ V_{2\mu'} = ig_{V_1K^*\bar{K}}\epsilon_{\alpha_1\beta_1\mu'\delta}p_1^{\alpha_1}p_{V_1}^{\beta_1}\varepsilon_{V_1}^{\delta*}, \\ V_{3\nu'} = ig_{V_2\bar{K}^*K}\epsilon_{\alpha_2\beta_2\nu'\lambda}p_3^{\alpha_2}p_{V_2}^{\beta_2}\varepsilon_{V_2}^{\lambda*}, \end{cases}$$

and the propagators for the vector and pseudoscalar mesons:

$$\begin{cases} D^{\mu\mu'}(K^*) = -i(g^{\mu\mu'} - p^\mu p^{\mu'}/p^2)/(p^2 - m_{K^*}^2 + i\epsilon) \\ D(K) = i/(p^2 - m_K^2 + i\epsilon) \end{cases}$$

A form factor is introduced to cut off the UV divergence:

$$\mathcal{F}(p_i^2) = \prod_i \left(\frac{\Lambda_i^2 - m_i^2}{\Lambda_i^2 - p_i^2}\right),$$

with $\Lambda_i \equiv m_i + \alpha\Lambda_{QCD}$, and $\Lambda_{QCD} = 220$ MeV, and $\alpha \simeq 1 \sim 2$.

3. Numerical results and discussions

in unit of $(\times 10^{-3})$

Process		[13]	[12]	[14]	[11]	[8]	[8]*	[9]	[10]	Our results *without* FSIs	Our results *with* FSIs	Experiments
$\phi\rho^0$	**S**	···	0.63	···	···	···	···	···	···	0.48	$1.35^{+0.23}_{-0.20}$	1.40 ± 0.12 [21]
	P	···	0.025	···	···	···	···	···	···	0.05	$0.11^{+0.04}_{-0.03}$	0.08 ± 0.04 [21]
	D	···	0.001	···	···	···	···	···	···	~0	$0.002^{+0.001}_{-0.001}$	0.08 ± 0.03 [21]
	T	···	···	···	···	···	···	···	···	0.37	$1.02^{+0.21}_{-0.18}$	···
	L	0.65 ± 0.04	···	···	···	···	···	···	···	0.16	$0.45^{+0.07}_{-0.06}$	···
	Total	···	0.66	7.6(0.4)	1.02	0.26(0.26)	0.038 ± 0.014	1.9 ± 0.5	0.22	0.53	$1.47^{+0.27}_{-0.24}$	1.56 ± 0.13 [21]
$\phi\omega$	T	···	···	···	···	···	···	···	···	0.34	$0.67^{+0.12}_{-0.10}$	0.65 ± 0.10 [20]
	L	1.41 ± 0.09	···	···	···	···	···	···	···	0.15	$0.03^{+0.001}_{-0.002}$	~0 [20]
	Total	···	0.66	···	0.92	0.23(0.23)	0.035 ± 0.13	···	···	0.49	$0.69^{+0.12}_{-0.10}$	0.65 ± 0.10 [20]

- The FSIs via $VV^{(DE)} \to VV^{(CS)}$ seems to be a natural explanation for the mysterious issues in $D^0 \to VV$, including the polarization puzzles.
- FSIs of the leading DE transitions can rescatter into the CS processes and produce significant interfering effects.
- The significant differences between the $\phi\rho^0$ and $\phi\omega$ decay channels can be understood.

4. Extension: $D^0 \to V\gamma$

- The radiative weak decay $D^0 \to V\gamma$ ($V = \bar{K}^{*0}, \phi, \rho^0, \omega$) can be related with the color-suppressed process in $D^0 \to VV$.
- The present experimental measurements of $D^0 \to V\gamma$.

  (BaBar, Belle and CLEO Collaboration)
- The previous work $D^0 \to VV$ suggests the weak decay mechanism and implies the importance of FSIs via rescatterings.

For B meson weak radiative decay:

the amplitude is dominated by the free quark decay, e.g. $b \to s\gamma$.

But this picture cannot be justified for $D \to V\gamma$.

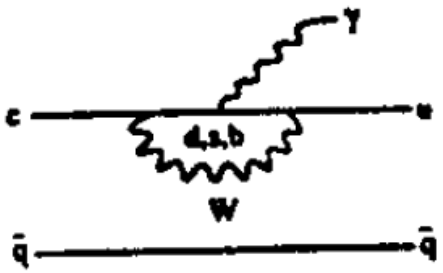

- The charm quark production and decay has been an ideal place for probing the non-pQCD effects

Formalism: CS-processes

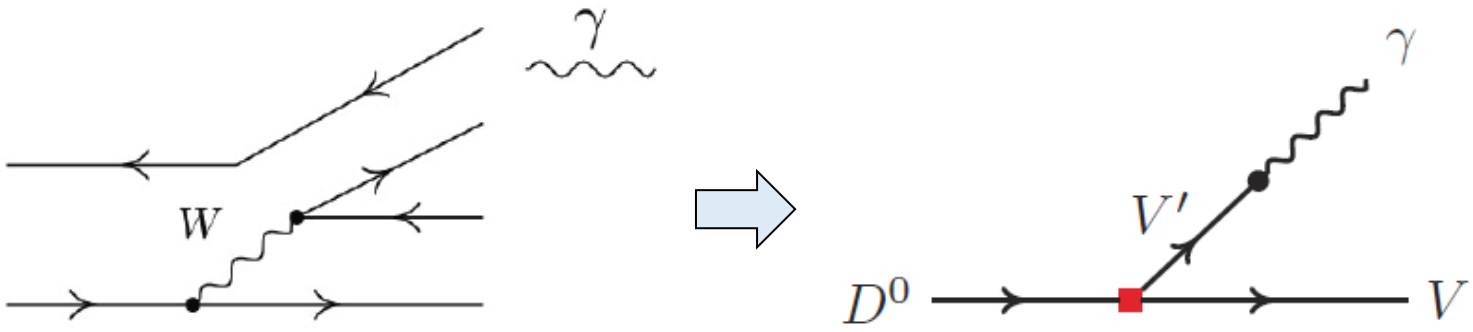

$$i\mathcal{M}^{(\mathrm{PC})}_{T(a)} = ig^{(\mathrm{PC})}_{DV\gamma}\epsilon_{\alpha\beta\delta\lambda}p^{\alpha}_{\gamma}p^{\beta}_{V}\varepsilon^{\delta}_{\gamma}\varepsilon^{\lambda}_{V},$$

$$i\mathcal{M}^{(\mathrm{PV})}_{T(a)} = -ig^{(\mathrm{PV})}_{DV\gamma}\varepsilon^{\mu}_{\gamma}\varepsilon_{V\mu},$$

where

$$g^{(\mathrm{P})}_{DV\gamma} = -ig^{(\mathrm{P})}_{DVV'}\frac{em^2_{V'}}{f_{V'}}G_{V'},$$

$$G_{V'} \equiv \frac{-i}{p^2_{\gamma} - m^2_{V'} + im_{V'}\Gamma_{V'}}$$

The internal W-emission process $c \to q_1\bar{q}_2q$, followed by $\bar{q}_2q \to \gamma$ (or $\bar{q}_1u \to \gamma$)

The vector meson dominance (VMD) model

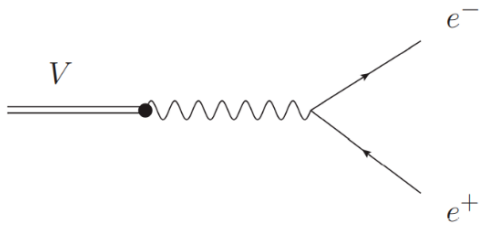

$$\mathcal{L}_{V\gamma} = \sum_{V}\frac{em^2_{V}}{f_{V}}V_{\mu}A^{\mu}$$

Bauer et al., Rev. Mod. Phys. 50 (1978), 261.

1. The photon interacts with hadrons by coupling via the vector mesons (ϕ, ρ^0, ω saturation).
2. The decay constant f_V can be determined by $V \to e^+e^-$ using the experimental data.

$$\frac{e}{f_V} = \left(\frac{3\Gamma_{V\to e^+e^-}}{2\alpha_e|\mathbf{p}_e|}\right)^{1/2}$$

3. $g^{(P)}_{DVV'}$ can be extracted from the CS transition in $D^0 \to VV$.

Formalism: pole terms

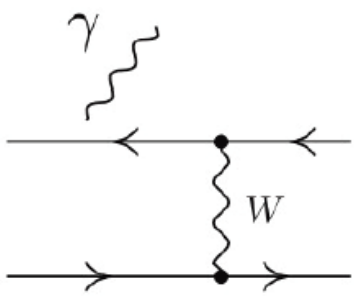

(b)

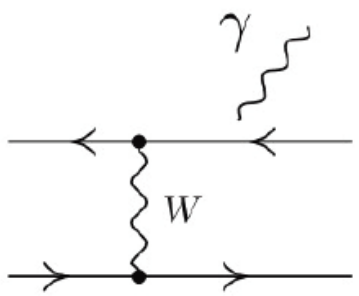

(c)

Type-I

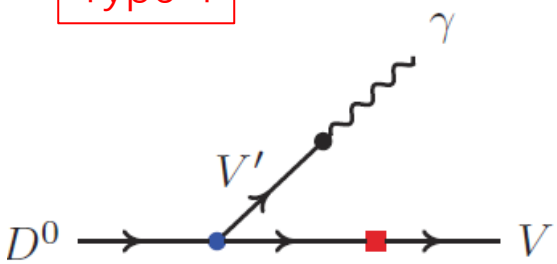

(b)

Type-II

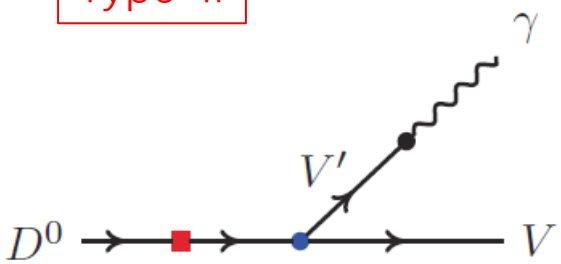

(c)

The internal conversion process $c\bar{u} \to q_1\bar{q}_2$ with a photon attached to any of the four quark lines.

All possible spin-one ($J^P = 1^{\pm}$) and spin-zero ($J^P = 0^{\pm}$) intermediate virtual particles can contribute.

$$\mathcal{M}_I^{(\mathrm{P})}(D \to V\gamma) = \sum_n \langle V|H_{W,2\to2}^{(\mathrm{P})} \frac{i}{m_V^2 - m_{D_n^*}^2 + i m_{D_n^*}\Gamma_{D_n^*}} |D_n^*\rangle\langle D_n^*|H_{EM}|D\rangle,$$

$$\mathcal{M}_{II}^{(\mathrm{P})}(D \to V\gamma) = \sum_n \langle V|H_{EM} \frac{i}{m_D^2 - m_{P_n}^2 + i m_{P_n}\Gamma_{P_n}} |P_n\rangle\langle P_n|H_{W,2\to2}^{(\mathrm{P})}|D\rangle.$$

only consider the **PC** contributions

- $g_{DD^*(1^-)V}$ can be extracted by the heavy quark effective theory.
- $g_{VVP(0^-)}$ can be extracted by fitting the $V \to P\gamma(P \to V\gamma)$ channels using the VMD model.
- We know little about the property of the D^0 couplings to the axial-vector meson $D_1(1^+)$ and a neutral vector meson.
- we also lack the coupling information for the intermediate scalar meson (0^+) transits into the vector meson pair.

TABLE VII: The b.r.s of the tree contributions shown in Fig. 2(a) and pole term contributions shown in Fig. 2(b) and (c) in units of 10^{-5} for the decay $D^0 \to V\gamma$ ($V = \bar{K}^{*0},\ \phi,\ \rho^0,\ \omega$).

b.r.		$\bar{K}^{*0}\gamma$	$\phi\gamma$	$\rho^0\gamma$	$\omega\gamma$
Experimental data [19]		41 ± 7	2.81 ± 0.19	1.82 ± 0.32	< 24
Tree	PC	11.03 ± 5	0.55 ± 0.23	0.45 ± 0.16	0.023 ± 0.020
	PV	12.53 ± 4	0.75 ± 0.25	0.45 ± 0.13	0.023 ± 0.016
	PC+PV	23.57 ± 6	1.30 ± 0.34	0.90 ± 0.21	0.047 ± 0.026
Pole terms	PC	0.011	0.016	0.055	0.005
Tree(PC+PV) + Pole terms(PC)		22.80	1.14	1.23	0.046

- The transition amplitudes of the two types of pole terms have opposite signs and will cancel with each other.
- We see that the cancellation has led to rather small effects on the b.r.s as shown in Tab. VII.
- We argue that the PV part of pole terms have the similar behaviors.

Formalism: loop amplitudes

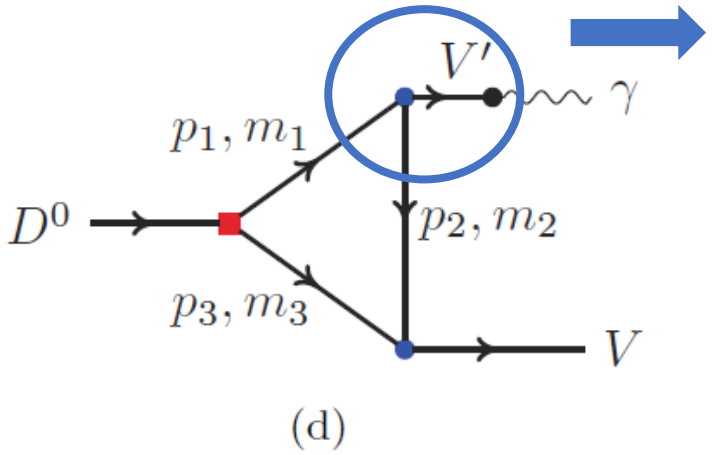

(d)

Taking the $K^{*+}K^-$ coupling to the photon γ as an example, the photon can couple to the intermediate ρ^0, ω, and ϕ meson:

$$g_{K^{*+}K^+\gamma} = \sum_{q=u,s} \sum_{V'=\rho^0,\omega,\phi} \langle (q\bar{q})_{1^{--}} | V' \rangle i g_{V'VP} \frac{e m_{V'}^2}{f_{V'}} G_{V'},$$

The expressions and numerical calculations of these loop amplitudes are the same as the above.

Numerical results and discussions

TABLE IX: Calculated b.r.s containing both tree and loop contributions in units of 10^{-5} for the four radiative weak decays $D^0 \to V\gamma$ $(V = \bar{K}^{*0}, \phi, \rho^0, \omega)$. The uncertainties are given by $\alpha = 1.3 \pm 0.13$.

	$D^0 \to \bar{K}^{*0}\gamma$	$D^0 \to \phi\gamma$	$D^0 \to \rho^0\gamma$	$D^0 \to \omega\gamma$
Experimental data	$32.8 \pm 2.0 \pm 2.7$ [4] $46.6 \pm 2.1 \pm 2.1$ [5]	$2.78 \pm 0.32 \pm 0.27$ [4] $2.76 \pm 0.19 \pm 0.10$ [5]	$1.77 \pm 0.30 \pm 0.07$ [5]	< 24 [3]
PDG average [19]	41 ± 7	2.81 ± 0.19	1.82 ± 0.32	< 24
Burdman [9]	$7 \sim 12$	$0.1 \sim 3.4$	$0.1 \sim 0.5$	~ 0.2
Biswas [12]	$4.6 \sim 18$	$0.48 \sim 0.64$	$0.512 \sim 1.8$	$0.32 \sim 0.9$
Fajfer [10]	$6 \sim 36$	$0.4 \sim 1.9$	$0.1 \sim 1$	$0.1 \sim 0.9$
Shen [13]	19^{+7+1}_{-6-1}	$3.2^{+1.3+0.3}_{-1.0-0.0}$	$1.1^{+0.4+0.1}_{-0.4-0.1}$	$0.75^{+0.30+0.05}_{-0.25-0.04}$
de Boer [11]	$2.6 \sim 46$	$0.24 \sim 2.8$	$0.041 \sim 1.17$	$0.042 \sim 1.12$
Asthana [6]	0.86	-	-	-
Bajc [8]	$28 \sim 65$	-	-	-
Dias [25]	$15.5 \sim 34.4$	-	-	-
This work	$35.9^{+2.0}_{-2.2}$	$2.76^{+0.36}_{-0.35}$	$1.79^{+0.24}_{-0.22}$	$0.58^{+0.14}_{-0.13}$

[9]PRD, 52:6383{6399, 1995.
[12] Int.J.Mod.Phys.A, 33(32):1850194, 2018..
[10] Eur.Phys.J.C, 6:471-476, 1999.
[13]Eur.Phys.J.C, 73:2441,2013.
[11]JHEP, 08:091,2017.
[6] PRD, 43:278{281, 1991.
[8] PRD, 51:2230-2236, 1995.
[25] Chin. Phys. C, 42(4):043106, 2018.

Branching ratios containing both tree and loop contributions.

- Our results for $D^0 \to \phi\gamma$ and $\rho^0\gamma$ with $\alpha = 1.3 \pm 0.13$ can best describe the experimental data from Belle [5] Collaboration.
- The calculated b.r. for $D^0 \to \bar{K}^{*0}\gamma$ is consistent with the averaged value of the BaBar [4] and Belle [5] measurements.
- The b.r. for $D^0 \to \omega\gamma$ is much smaller than the experimental upper limit from the CLEO Collaboration [3].

Summary

- In the first work, we carry out a systematic analysis of the CF and SCS decays of $D^0 \to VV$ by taking into account the long-distance FSIs as a crucial mechanism for understanding the mysterious polarization puzzles.
- We also strongly recommend future precise and completed measurements of $D^0 \to VV$ at BESIII, since it will provide us a unique probe for resolving some of those profound nonperturbative dynamics.
- We demonstrate that the long-distance FSIs also have played a crucial role in understanding the $D^0 \to V\gamma$ decays.
- This mechanism may be investigated in other decay channels and help us gain better insights into the near-threshold dynamics in charm sector via the weak transitions.

Thanks for your attention!

Backup

Tree-level amplitudes in the NRCQM

The tree-level amplitudes will be calculated in the non-relativistic constituent quark model (NRCQM):

The effective weak Hamiltonian: $$H_W = \frac{G_F}{\sqrt{2}} \int \mathrm{d}\boldsymbol{x}\, \frac{1}{2}\{J^{-,\mu}(\boldsymbol{x}), J^{+}_{\mu}(\boldsymbol{x})\},$$

where
$$\begin{cases} J^{+,\mu}(\boldsymbol{x}) = (\bar{u} \;\; \bar{c}) \cdot \gamma^{\mu}(1-\gamma_5) \cdot \begin{pmatrix} \cos\theta_C & -\sin\theta_C \\ \sin\theta_C & \cos\theta_C \end{pmatrix} \cdot \begin{pmatrix} d \\ s \end{pmatrix}, \\ J^{-,\mu}(\boldsymbol{x}) = (\bar{d} \;\; \bar{s}) \cdot \begin{pmatrix} \cos\theta_C & -\sin\theta_C \\ \sin\theta_C & \cos\theta_C \end{pmatrix} \cdot \gamma^{\mu}(1-\gamma_5) \cdot \begin{pmatrix} u \\ c \end{pmatrix}. \end{cases}$$

The operators for the W emission and internal W exchange are:

$$\begin{aligned} H_{W,1\to3} &= \frac{G_F}{\sqrt{2}} V_{q_2 q_2'} V_{q_3 q_4} \frac{1}{(2\pi)^3} \delta^3(\boldsymbol{p}_2 - \boldsymbol{p}_2' - \boldsymbol{p}_3 - \boldsymbol{p}_4) \\ &\quad \times \bar{u}(\boldsymbol{p}_2', m_2')\gamma_\mu(1-\gamma_5)u(\boldsymbol{p}_2, m_2)\bar{u}(\boldsymbol{p}_4, m_4)\gamma^\mu(1-\gamma_5)v(\boldsymbol{p}_3, m_3), \\ H_{W,2\to2} &= \frac{G_F}{\sqrt{2}} V_{q_2 q_2'} V_{q_1 q_1'} \frac{1}{(2\pi)^3} \delta^3(\boldsymbol{p}_1 + \boldsymbol{p}_2 - \boldsymbol{p}_1' - \boldsymbol{p}_2') \\ &\quad \times \bar{u}(\boldsymbol{p}_2', m_2')\gamma_\mu(1-\gamma_5)u(\boldsymbol{p}_2, m_2)\bar{v}(\boldsymbol{p}_1, m_1)\gamma^\mu(1-\gamma_5)v(\boldsymbol{p}_1', m_1). \end{aligned}$$

A. Le Yaouanc, L. Oliver, O. Pene, and J. C. Raynal. HADRON TRANSITIONS IN THE QUARK MODEL. 1988

For instance, the operators for the W-emission $(1 \to 3)$ in the PC and PV transitions:

$$H^{PC}_{W,1\to3} = \frac{G_F}{\sqrt{2}} V_{q_2 q_2'} V_{q_3 q_4} \frac{\beta}{(2\pi)^3} \delta^3(\boldsymbol{p}_2 - \boldsymbol{p}_2' - \boldsymbol{p}_3 - \boldsymbol{p}_4) \hat{O}_{color} \hat{O}_{flavor}$$
$$\times \{\langle s_2'|I|s_2\rangle \langle s_4\bar{s}_3|\boldsymbol{\sigma}|0\rangle \cdot (\frac{\boldsymbol{p}_3}{2m_3} + \frac{\boldsymbol{p}_4}{2m_4}) + \langle s_2'|\boldsymbol{\sigma}|s_2\rangle \cdot (\frac{\boldsymbol{p}_2}{2m_2} + \frac{\boldsymbol{p}_2'}{2m_2'}) \langle s_4\bar{s}_3|I|0\rangle$$
$$- \langle s_4\bar{s}_3|\boldsymbol{\sigma}|0\rangle \cdot [\langle s_2'|I|s_2\rangle (\frac{\boldsymbol{p}_2}{2m_2} + \frac{\boldsymbol{p}_2\prime}{2m_2'}) - i\langle s_2'|\boldsymbol{\sigma}|s_2\rangle \times (\frac{\boldsymbol{p}_2}{2m_2} - \frac{\boldsymbol{p}_2'}{2m_2'})]$$
$$- \langle s_2'|\boldsymbol{\sigma}|s_2\rangle \cdot [(\frac{\boldsymbol{p}_3}{2m_3} + \frac{\boldsymbol{p}_4}{2m_4}) \langle s_4\bar{s}_3|I|0\rangle - i\langle s_4\bar{s}_3|\boldsymbol{\sigma}|0\rangle \times (\frac{\boldsymbol{p}_3}{2m_3} - \frac{\boldsymbol{p}_4}{2m_4})]\},$$

$$H^{PV}_{W,1\to3} = \frac{G_F}{\sqrt{2}} V_{q_2 q_2'} V_{q_3 q_4} \frac{\beta}{(2\pi)^3} \delta^3(\boldsymbol{p}_2 - \boldsymbol{p}_2' - \boldsymbol{p}_3 - \boldsymbol{p}_4) \hat{O}_{color} \hat{O}_{flavor}$$
$$\times \{-\langle s_2'|I|s_2\rangle \langle s_4\bar{s}_3|I|0\rangle + \langle s_2'|\boldsymbol{\sigma}|s_2\rangle \cdot \langle s_4\bar{s}_3|\boldsymbol{\sigma}|0\rangle\},$$

The breaking of the SU(3) flavor symmetry will arise partially from the quark model wave functions due to the quark mass difference.

- A. Le Yaouanc, L. Oliver, O. Pene, and J. C. Raynal. HADRON TRANSITIONS IN THE QUARK MODEL. 1988
- J.-M. Richard, Q. Wang, and Q. Zhao, arXiv:1604.04208[nucl-th]
- P.-Y. Niu, J.-M. Richard, Q. Wang, and Q. Zhao, Phys. Rev. D102, 073005 (2020)
- P.-Y. Niu, Q. Wang, and Q. Zhao, Phys. Lett. B 826 (2022) 136916

VV modes	BR of DE	$g_{\mathrm{DE}}^{(\mathrm{PC})}(\mathrm{GeV}^{-1})$	$g_{\mathrm{DE}}^{(\mathrm{PV})}$ (GeV)
$K^{*-}\rho^{+}$	0.22 ± 0.06	2.61 ± 0.43	4.90 ± 0.63
$K^{*+}K^{*-}$	$(0.89 \pm 0.29)\%$	2.91 ± 0.60	5.45 ± 0.89
$\rho^{+}\rho^{-}$	$(1.33 \pm 0.49)\%$	2.96 ± 0.88	4.74 ± 0.80

Couplings are determined by the NRCQM.

PP/VP modes	BR of experiment	$g^{(\mathrm{PC})}$	$g^{(\mathrm{PV})}$ (GeV)
$K^{-}\pi^{+}$	$(3.95 \pm 0.03)\%$	0	2.64 ± 0.01
$K^{+}K^{-}$	$(4.08 \pm 0.06) \times 10^{-3}$	0	3.84 ± 0.03
$\pi^{+}\pi^{-}$	$(1.45 \pm 0.02) \times 10^{-3}$	0	2.19 ± 0.02
$K^{*-}\pi^{+}$	$(6.93 \pm 1.20)\%$	1.29 ± 0.11	0
$\rho^{+}K^{-}$	$(11.20 \pm 0.70)\%$	1.54 ± 0.05	0
$K^{*-}K^{+}$	$(1.86 \pm 0.30) \times 10^{-3}$	1.16 ± 0.09	0
$K^{*+}K^{-}$	$(5.67 \pm 0.90) \times 10^{-3}$	2.02 ± 0.16	0
$\rho^{-}\pi^{+}$	$(5.15 \pm 0.25) \times 10^{-3}$	1.23 ± 0.03	0
$\rho^{+}\pi^{-}$	$(1.01 \pm 0.04)\%$	1.72 ± 0.03	0

Couplings are determined by the experimental data.

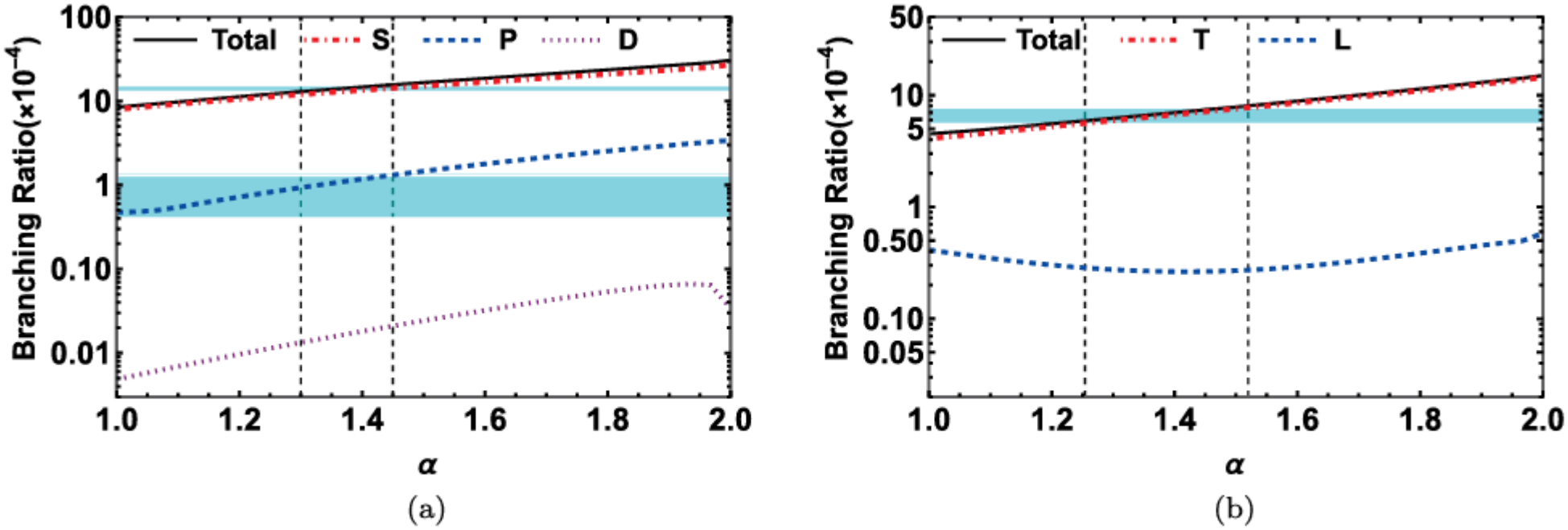

FIG. 2. Cutoff parameter α dependence of (a) the partial-wave BRs of $D^0 \to \phi\rho^0$ and (b) polarization BRs of $\phi\omega$, respectively. The solid lines stand for the total BRs The partial-wave and polarization BRs are denoted by the line legends.

Form factor : $\mathcal{F}(p_i^2) = \prod_i (\frac{\Lambda_i^2 - m_i^2}{\Lambda_i^2 - p_i^2})$, with $\Lambda_i \equiv m_i + \alpha\Lambda_{QCD}$, and $\Lambda_{QCD} = 220$ MeV, and $\alpha \simeq 1 \sim 2$.

TABLE III: The tree-level amplitudes of all the Cabibbo-favored and singly Cabibbo-suppressed radiative weak decay channels for $D^0 \to V\gamma$ ($V = \bar{K}^{*0},\ \phi,\ \rho^0,\ \omega$). (Note that: there is no CS-process in $D^0 \to \rho^0\omega$.)

Modes	Tree amplitudes (Fig. 2(a))
$\bar{K}^{*0}\gamma$	$\frac{1}{\sqrt{2}}g^{(\mathrm{P})}_{W(\mathrm{CS})}V_{cs}V_{ud}\frac{em^2_{\rho^0}}{f_{\rho^0}}G_{\rho^0} + \frac{1}{\sqrt{2}}g^{(\mathrm{P})}_{W(\mathrm{CS})}V_{cs}V_{ud}\frac{em^2_{\omega}}{f_{\omega}}G_{\omega}$
$\phi\gamma$	$\frac{1}{\sqrt{2}}g^{(\mathrm{P})}_{W(\mathrm{CS})}V_{cs}V_{us}\frac{em^2_{\rho^0}}{f_{\rho^0}}G_{\rho^0} + \frac{1}{\sqrt{2}}g^{(\mathrm{P})}_{W(\mathrm{CS})}V_{cs}V_{us}\frac{em^2_{\omega}}{f_{\omega}}G_{\omega}$
$\rho^0\gamma$	$-\frac{1}{2}g^{(\mathrm{P})}_{W(\mathrm{CS})}V_{cd}V_{ud}\frac{em^2_{\rho^0}}{f_{\rho^0}}G_{\rho^0} + \frac{1}{\sqrt{2}}g^{(\mathrm{P})}_{W(\mathrm{CS})}V_{cs}V_{us}\frac{em^2_{\phi}}{f_{\phi}}G_{\phi}$
$\omega\gamma$	$\frac{1}{2}g^{(\mathrm{P})}_{W(\mathrm{CS})}V_{cd}V_{ud}\frac{em^2_{\omega}}{f_{\omega}}G_{\omega} + \frac{1}{\sqrt{2}}g^{(\mathrm{P})}_{W(\mathrm{CS})}V_{cs}V_{us}\frac{em^2_{\phi}}{f_{\phi}}G_{\phi}$

TABLE II: Vector meson decay constants determined by $V' \to e^+e^-$. The data are taken from the PDG [19].

Channel	Total width of V'	BR($V' \to e^+e^-$)	$e/f_{V'}(\times 10^{-2})$
$\phi \to e^+e^-$	4.25 MeV	$(2.98 \pm 0.03) \times 10^{-4}$	-2.26
$\rho^0 \to e^+e^-$	147.4 MeV	$(4.72 \pm 0.05) \times 10^{-5}$	6.07
$\omega \to e^+e^-$	8.68 MeV	$(7.38 \pm 0.22) \times 10^{-5}$	1.83
$J/\psi \to e^+e^-$	92.6 keV	$(5.97 \pm 0.032)\%$	2.71

To obtain the EM transition matrix elements, we describe the electromagnetic vertices in the VMD model.

$$g_{D^0D^{*0}\gamma} = ig_{\rho^0 D^0 \bar{D}^{*0}} \frac{em_{\rho^0}^2}{f_{\rho^0}} G_{\rho^0} + ig_{\omega D^0 \bar{D}^{*0}} \frac{em_{\omega}^2}{f_{\omega}} G_{\omega} + ig_{J/\psi D^0 \bar{D}^{*0}} \frac{em_{J/\psi}^2}{f_{J/\psi}} RG_{J/\psi},$$

Electromagnetic couplings	Values in VMD (Magnitude)	Experimental values
$g_{K^+K^{*+}\gamma}$ [GeV^{-1}]	$-0.288 - 0.063i$ (0.294)	-0.253 ± 0.012
$g_{K^0K^{*0}\gamma}$ [GeV^{-1}]	$0.369 + 0.062i$ (0.374)	0.385 ± 0.016
$g_{K^{*+}K^{*+}\gamma}$	$0.324 + 0.036i$ (0.326)	e
$g_{K^{*0}K^{*0}\gamma}$	$-0.046 - 0.034i$ (0.057)	0
$g_{K^+K^+\gamma}$	$0.324 + 0.036i$ (0.326)	e
$g_{K^0K^0\gamma}$	$-0.046 - 0.034i$ (0.057)	0
$g_{\pi^+\rho^+\gamma}$ [GeV^{-1}]	$-0.205 - 0.002i$ (0.205)	-0.219 ± 0.012
$g_{\pi^0\rho^0\gamma}$ [GeV^{-1}]	$-0.205 - 0.002i$ (0.205)	-0.222 ± 0.019
$g_{\rho^+\rho^+\gamma}$	$0.347 + 0.066i$ (0.354)	e
$g_{\rho^0\rho^0\gamma}$	0	0
$g_{\pi^+\pi^+\gamma}$	$0.347 + 0.066i$ (0.354)	e
$g_{\pi^0\pi^0\gamma}$	0	0
$g_{\eta\phi\gamma}$ [GeV^{-1}]	$-0.192 - 0.0008i$ (0.192)	-0.209 ± 0.002
$g_{\eta'\phi\gamma}$ [GeV^{-1}]	$0.213 + 0.0009i$ (0.213)	0.217 ± 0.004
$g_{\eta\rho^0\gamma}$ [GeV^{-1}]	$-0.488 - 0.093i$ (0.496)	-0.478 ± 0.017
$g_{\eta'\rho^0\gamma}$ [GeV^{-1}]	$-0.440 - 0.084i$ (0.447)	-0.434 ± 0.003
$g_{\eta\omega\gamma}$ [GeV^{-1}]	$-0.152 - 0.002i$ (0.152)	-0.136 ± 0.006
$g_{\eta'\omega\gamma}$ [GeV^{-1}]	$-0.137 - 0.002i$ (0.137)	-0.134 ± 0.002
$g_{\pi^0\omega\gamma}$ [GeV^{-1}]	$-0.657 - 0.125i$ (0.669)	-0.707 ± 0.011
$g_{D^0D^{*0}\gamma}$ [GeV^{-1}]	$-0.389 - 0.053i$ (0.393)	> -3.297

R is an SU(4) flavor symmetry breaking parameter and it distinguishes the production of a $c\bar{c}$ from that of $u\bar{u}(d\bar{d})$.

$R \approx \frac{f_\pi}{f_{c\bar{c}}} \approx \frac{132}{487.4} \approx 0.27.$

(T. Peng and B. Q. Ma, PRD84, 034003 (2011))

In the last column the signs of the values are determined in the quark level, which is consistent with the relative signs of their values in the VMD model.

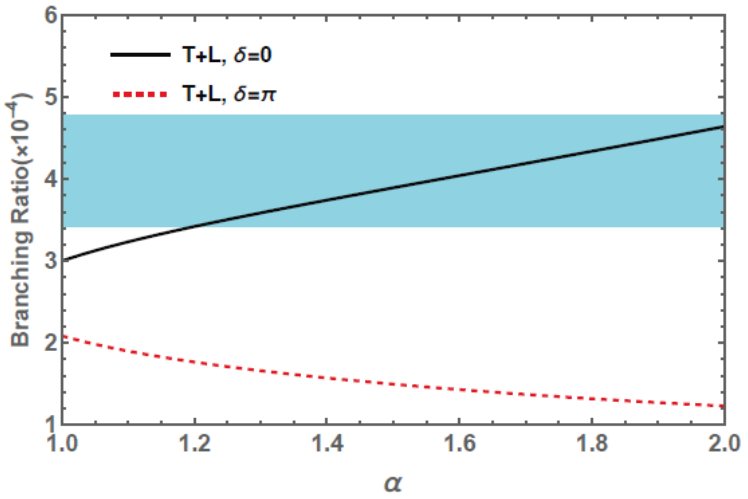

(a) $D^0 \to \bar{K}^{*0}\gamma$

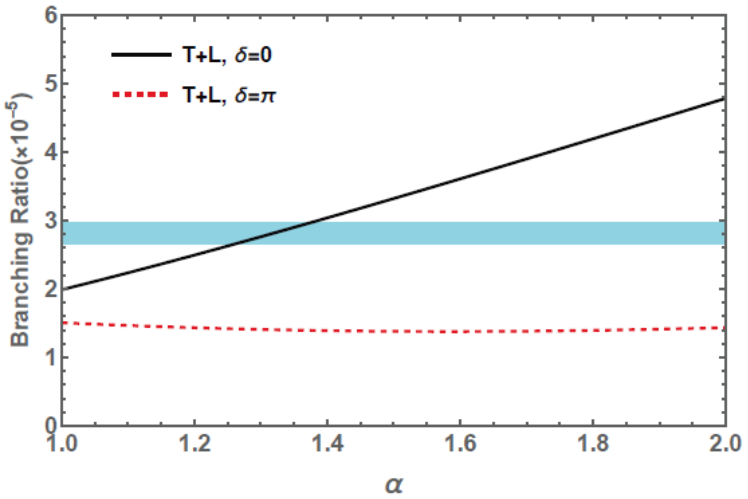

(b) $D^0 \to \phi\gamma$

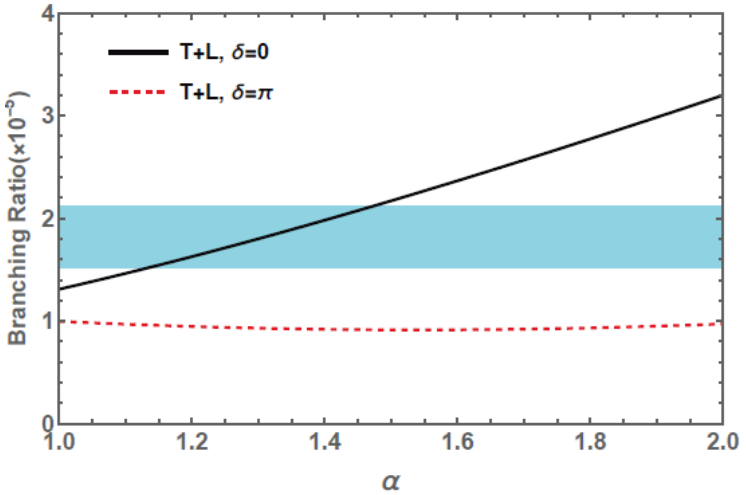

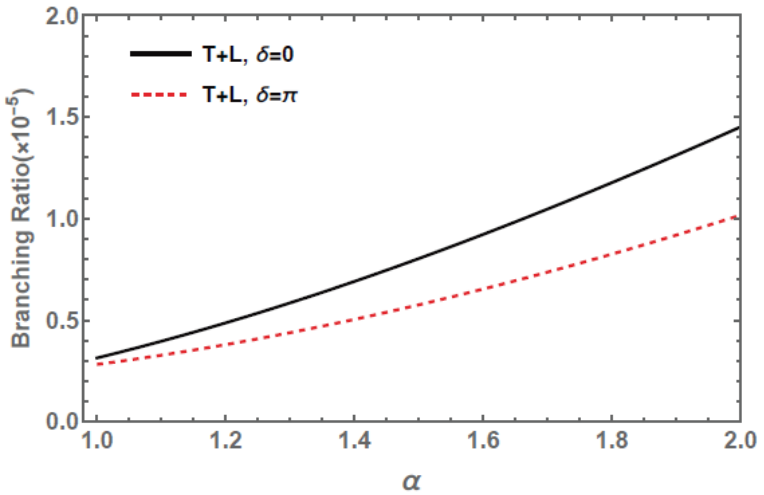

- We plot the cut-off parameter α dependence of the b.r.s. to see the role played by the FSIs.

(The horizontal bands are the PDG average of the experimental measurements.)

- We find that the data for $D^0 \to \bar{K}^{*0}\gamma, \phi\gamma, \rho^0\gamma$ can be accounted for within a range of $\alpha = 1.3 \pm 0.13$ with $\delta = 0$.